[10] Jocelyn Lawrence, A. and Jackson, P., "Comparison of Different Methods of Assessing the Free Oscillatory Characteristics of Aeroelastic Systems," British Aeronautical Research Council, C.P. No. 1084, 1970.
[11] Woodcock, D.L. and Jocelyn Lawrence, A., "Further Comparisons of Different Methods of Assessing the Free Oscillatory Characteristics of Aeroelastic Systems," Royal Aircraft Establishment, Tech. Rept. 72188, Sept. 1972.
[12] Rodden, W.P., Harder, R.L., and Bellinger, E.D., "Aeroelastic Addition to NASTRAN," NASA CR 3094, 1979.
[13] Bisplinghoff, R.L., Ashley, H., and Halfman, R.L., *Aeroelasticity*, Addison-Wesley, Reading, Mass., 1955.
[14] Jones, W.P., "Aerodynamic Forces on Wings in Non-Uniform Motion," British Aeronautical Research Council, R&M 2117, 1945.
[15] Fung, Y.C., *An Introduction to the Theory of Aeroelasticity*, John Wiley and Sons, New York, 1955, p. 215.
[16] Rodden, W.P. and Harder, R.L., "Flutter Analysis with Active Controls," Paper presented at the MSC/NASTRAN User's Conference, Pasadena, Calif., Jan. 1975.
[17] Armstrong, E.S., "ORACLS—A System for Linear-Quadratic-Gaussian Control Law Design," NASA TP-1106, April 1978.
[18] Mahesh, J.K., Stone, C.R., Garrard, W.L., and Dunn, H.J., "Control Law Synthesis for Flutter Suppression Using Linear Quadratic Gaussian Theory," *Journal of Guidance and Control*, Vol. 4, July-Aug. 1981, pp. 415-422.

AIAA 81-1944R

Stress Measurements in a Ribbon Parachute Canopy

Thomas A. Konicke*
U.S. Air Force, Edwards Air Force Base, Calif.
and
William L. Garrard†
University of Minnesota, Minneapolis, Minn.

Nomenclature

F = drag force
n = $(\sigma_{max}/\sigma_{ss})(F_{ss}/F_{max})$
R = nominal radius
S = distance from apex measured along gore centerline
S^* = nondimensional distance, S/R
t^* = ratio of time of maximum stress to time of maximum drag
σ = stress

Subscripts

max = maximum
ss = steady state

Introduction

THE objective of this study was to experimentally determine the distribution of circumferential stress in a ribbon parachute canopy during inflation and at steady state. Stress measurements have been previously reported for block-[1,2] and bias-constructed,[3,4] flat, solid parachutes and for ringslot parachutes[2,5]; but not for ribbon parachutes. Stresses were measured on a circular, flat, block-constructed ribbon parachute model of 20% geometric porosity. Omega sensors[6] were mounted along the centerline of one of the gores in order to measure the distribution of circumferential stresses in the horizontal ribbons. Omega sensors were also mounted in different gores on the same ribbon in order to obtain the variation in stress from gore to gore. Additional Omega sensors were mounted across the slots to measure the force in the vertical tapes.

Parachute Design and Test Procedure

The parachute model used had a nominal diameter of 4.64 ft (1.43 m) and was constructed with 24 gores. The parachute was cut from 1.1 oz/yd^2 (37.4 g/m^2) rip stop nylon cloth which had an effective porosity of 4%. A hot knife was used to cut slots in the cloth in order to simulate the ribbons in a full-scale parachute. A total of 27 horizontal ribbons was simulated. Each gore contained four vertical tapes. Radial tapes were fabricated from the same material as the canopy and no pocket bands were used. The parachute was very flexible and exhibited a stable trim angle of attack of 0 deg.

Omega sensors were mounted on the outside of the parachute canopy. Six sensors were mounted at an S^* of 0.63 at the centerlines of every fourth gore in order to measure variations in circumferential stress from gore to gore. Ten additional sensors were mounted at S^* values of 0.19, 0.26, 0.33, 0.41, 0.48, 0.56, 0.70, 0.78, 0.85, and 0.93 at the centerline of gore 1 to obtain the circumferential stresses in the horizontal ribbons. Sensors were mounted between horizontal ribbons at S^* values of 0.44 and 0.77 to measure the force in the vertical tapes.

Wind tunnel tests were conducted in the same manner as in Ref. 4. It is important to note that the Omega sensors were calibrated after attachment to the parachute.

Results

A typical time history of three stresses and overall force for a test at 4.16 psf is given in Fig. 1. The power spectral density of the steady-state stress was measured at various values of dynamic pressure and, as shown in Ref. 7, there was no value of frequency other than zero at which the stress exhibited significant peaks. A hot wire anemometer showed large fluctuations in velocity outside the canopy near the Omega sensors. The power spectral density of the velocity fluctuations was relatively flat and had about the same bandwidth as the stress fluctuations. Thus it appears that the stress fluctuations resulted from turbulence rather than from some type of aeroelastic instability.

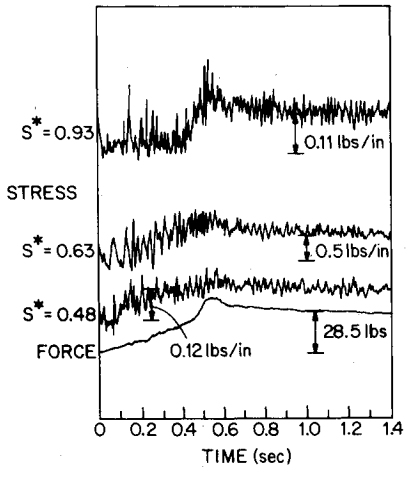

Fig. 1 Typical time history of stress and drag force.

Received Oct. 14, 1981; presented as Paper 81-1944 at the AIAA 7th Aerodynamic Decelerator and Balloon Technology Conference, San Diego, Calif., Oct. 21-23, 1981; revision received March 29, 1982.

*Second Lieutenant. Member AIAA.
†Associate Professor, Department of Aerospace Engineering and Mechanics. Associate Fellow AIAA.

Table 1 Gorewise variation in stress at $S^* = 0.6$

	Solid, flat parachute (orange)	Ribbon parachute
Mean value of normalized stress averaged across gores	0.918	1.099
Standard deviation of normalized stress across gores	0.226	0.063

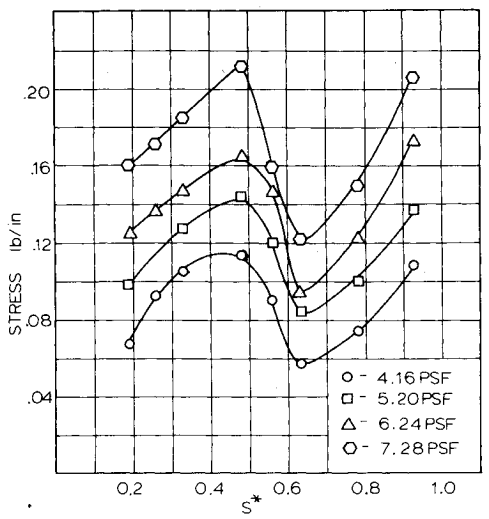

Fig. 2 Averaged steady-state stress distribution at four values of dynamic pressure.

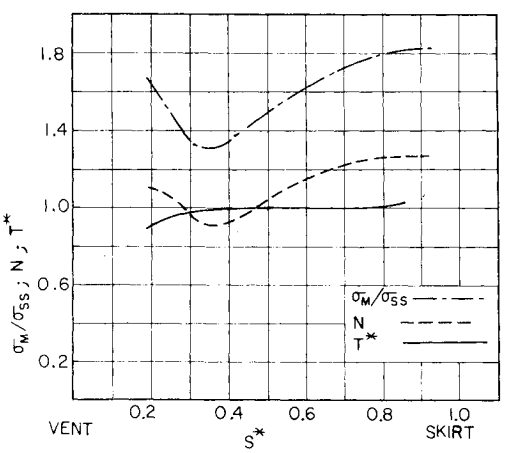

Fig. 3 Ratio of time of maximum stress to time of maximum drag; ratio of maximum stress to steady-state stress; and n factor vs S^*.

Table 2 Forces measured in vertical tapes and horizontal ribbons

q, psf	S^*	Vertical force, lb	Horizontal force, lb
4.16	0.44	0.05	0.11
4.16	0.77	0.04	0.08
5.20	0.44	0.06	0.14
5.20	0.77	0.05	0.10
6.28	0.44	0.08	0.17
6.28	0.77	0.06	0.12

The gorewise variations in steady-state stress are summarized in Table 1. Stresses were normalized with respect to the stress in gore 1 so a comparison could be made with measurements made on bias-constructed, flat, solid parachutes.[4] The standard deviation of the mean values of the normalized stress in each gore was much smaller in the ribbon parachute than in either of the solid parachutes.

The steady-state distribution of circumferential stress measured at four values of dynamic pressures is shown in Fig. 2. At each dynamic pressure the steady-state stress increased from the vent to a maximum about halfway between the vent and the skirt, rapidly decreased, and then increased to another maximum near the skirt. The average of the ratio of maximum stress during inflation to steady-state stress values of dynamic pressure is presented in Fig. 3. This ratio was essentially independent of dynamic pressure over the range tested. The ratio increased toward the skirt but to a much smaller degree than for the solid parachutes described in Ref. 4.

As in previous studies,[2,4] an n factor was used to examine the relationship between maximum force and maximum stress during inflation. If the maximum stress is only a function of maximum force during inflation, n would be 1. The value of n as a function of S^* is presented in Fig. 3. It can be seen that the maximum value of n occurs near the skirt; however, n is never greater than 1.25. A similar result has been reported for ringslot parachutes.[2] These results contrast sharply with those for solid parachutes for which n values of approximately 2.5 have been reported.[2,4] This indicates that dynamic effects not directly related to maximum opening force have a much greater affect on stresses in solid parachute canopies than in slotted canopies. In fact, multiplication of the steady-state stresses by the opening shock factor (F_{max}/F_{ss}) will give a reasonable estimate of maximum canopy stresses for slotted parachutes. This is not true for solid parachutes.

Figure 3 also presents the ratio of time of maximum stress to time of maximum overall drag as a function of S^*. The maximum stress near the vent occurs before the maximum force, whereas the maximum stress near the skirt occurs at about the same time as the maximum drag. This was explained by high-speed movies which revealed the vent area inflated considerably earlier than the skirt. Identical results have been reported for ringslot parachutes.[2,5] In solid parachutes, the maximum stress occurs before the maximum drag.[2,4] These differences indicate that dynamic effects due to rapid radial deceleration of the canopy, suspension lines, and included air mass have a much greater affect on the stress in solid parachutes than slotted parachutes. Radial deceleration would be expected to be much greater in solid parachutes owing to their shorter opening time compared with slotted parachutes. The ribbon parachute in this study inflated in 0.8 s while the 4-ft-diam solid parachutes of Ref. 4 inflated in 0.3 s.

Omega sensors were attached between horizontal ribbons at S^* values of 0.44 and 0.77, replacing one of the vertical tapes connecting the horizontal ribbons. The sensors measured the load carried by the vertical tapes which they replaced. The force in the vertical tapes are given in Table 2 along with the force in the horizontal ribbons at the same location.

Conclusions

Stress measurements are much easier to perform on ribbon parachutes than on solid parachutes. Experiments are much more repeatable, and few difficulties are encountered with Omega sensor failures during inflation. This is largely due to the slower opening characteristics of ribbon parachutes. In addition, the circumferential variation of steady-state stress at a given radial distance from the gore and the overall fluctuation of stress with time are much less in ribbon parachutes than in solid parachutes. It is felt that this is due to the fact that the flowfield around ribbon parachutes is much more uniform and less turbulent than the flowfield around solid parachutes.

Both the distribution of maximum stress during inflation and the steady-state stress distribution exhibit a peak about halfway between the vent and the skirt and a maximum value near the skirt. Both Heinrich and Saari[2] and Wagner[5] have reported maximum values of stress near the skirt for ringslot parachutes, but the intermediate peak has not been observed on ringslot parachutes. The ratio of maximum to steady-state stress ranges from about 1.25 to 1.75 with the maximum value occurring near the skirt and the minimum occurring at about 30% of the distance from the apex to the skirt. The ratio of maximum stress to steady-state stress is essentially constant with dynamic pressure and is much smaller in slotted parachutes than in solid parachutes.

Acknowledgment

This research was supported by Sandia National Laboratory, Albuquerque, N.Mex., under Contract 13-9879.

References

[1] Heinrich, H.G. and Noreen, R.A., "Stress Measurements on Inflated Parachute Models," AIAA Paper 73-445, May 1973.

[2] Heinrich, H.G. and Saari, D.G., "Parachute Canopy Stress Measurements at Steady State and During Inflation," *Journal of Aircraft*, Vol. 15, Aug. 1978, pp. 534-539.

[3] Heinrich, H.G., "Biaxial Stress Measurements on Cloth Samples and Bias Constructed Parachute Models," *Journal of Aircraft*, Vol. 17, July 1980, pp. 487-492.

[4] Garrard, W. L. and Konicke, T.A., "Stress Measurements in Bias-Constructed Parachute Canopies During Inflation and at Steady-State," *Journal of Aircraft*, Vol. 18, Oct. 1981, pp. 881-886.

[5] Wagner, P.M., "Experimental Measurement of Parachute Canopy Stress During Inflation," Tech. Rept. AFFDL-TR-78-53, May 1978.

[6] Braun, G. and Doherr, K.F., "Experiments with Omega Sensors for Measuring Stress in the Flexible Material of Parachute Canopies," *Journal of Aircraft*, Vol. 17, April 1980, pp. 358-364.

[7] Konicke, T.A. and Garrard, W.L., "Stress Measurements in a Ribbon Parachute Canopy During Inflation and at Steady State," AIAA Paper 81-1944, Oct. 1981.

AIAA 81-1949R

Development of the ARIES Parachute System

W.B. Pepper*
Sandia National Laboratories, Albuquerque, N. Mex.
and
F. M. Collins†
NASA Goddard Space Flight Center, Greenbelt, Md.

Introduction

ARIES is an attitude controlled sounding rocket used by NASA in support of its Space Sciences Physics and Astronomy Program. Following motor burnout, the payload follows a ballistic trajectory with approximately 8 min above the atmosphere. A parachute system is used to recover the payload after it re-enters the atmosphere at Mach 7 and slows down owing to aerodynamic drag. To develop the parachute recovery system,[1-3] an economical drop test vehicle was used. This 2000-lb vehicle could be loaded under the wing of a Navy A7 aircraft and dropped from 18,000 ft altitude.

Recovery System

The recovery system shown in Fig. 1 consists of a 15-ft-diam ribbon parachute reefed to 50% for 10 s and a 73-ft-diam paraform (cross) type second-stage parachute deployed 21 s after first-stage deployment. This parachute was reefed to 20% for 10 s.

Deployment Sequence

For the parachute development drop tests, a mechanical clock timer was used to deploy the parachute 2 s after release from the A7 aircraft at an altitude of 18,000 ft. Pullout wires extracted at release started the timer. The timer transmitted a 30-V signal to the pressure cartridges in the two six-ball thrusters located at the aft end of the vehicle. The 4.81-lb lid was ejected at 74 ft/s, deploying the reefed drogue chute.

The drogue loads were transmitted into the structure by a load plate which was held in the canister by a ball-locking mechanism. At the preset time (21 s), the mechanical timer fired the pyrotechnic pressure cartridges in two pin pushers. These unlocked the ball-locking mechanisms and released the load plate. The main canopy bag was attached to the load plate by a four-leg bridle.

For two ARIES rocket-launched operational flights, the deployment sequence was initiated after re-entry at Mach 7 by a barometric switch set to activate the same thrusters used for the drop tests and deploy the lid at 18,000 ft.

Results

Two successful drop tests of the final parachute system were conducted. The second test was a 20% overtest in dynamic pressure at lid fire and 12% in vehicle weight to qualify the recovery system for operational rocket flight. It should be noted that both chutes used in the first test were repacked and used on the second test without any damage.

Two operational recoveries of NASA telescope payloads were conducted successfully. Payload weights were 1600 and 2056 lb. The 44-in.-diam by 15.8-ft-long cylindrical payloads re-enter the atmosphere at about Mach 7 with the parachute compartment lid on the end of the payload facing the oncoming airflow. A cork insulating layer on the forward end of the payload was charred black from aerodynamic heating. The payloads were recovered undamaged with the impact velocity being approximately 30 ft/s.

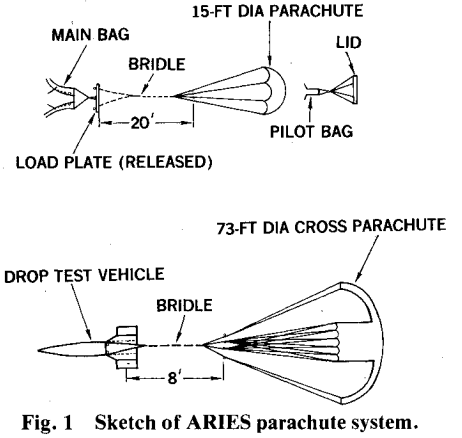

Fig. 1 Sketch of ARIES parachute system.

Received Oct. 14, 1981; presented as Paper 81-1949 at the AIAA 7th Aerodynamic Decelerator and Balloon Technology Conference, San Diego, Calif., Oct. 21-23, 1981; revision received Feb. 22, 1982. This paper is declared a work of the U.S. Government and therefore is in the public domain.

*Member of Technical Staff, Aerodynamics Department. Associate Fellow AIAA.

†Head of Advanced Vehicles Section, Flight Performance Branch of the Sounding Rockets Division. Member AIAA.